An experimental study on single drop rising in a low interfacial tension liquid-liquid system

Jiyizhe Zhang[1], Yundong Wang*[1], Geoffrey W. Stevens[2], Weiyang Fei[1]
[1] The State Key Laboratory of Chemical Engineering, Department of Chemical Engineering, Tsinghua University, Beijing 100084, China,
[2] Department of Chemical and Biomolecular Engineering, The University of Melbourne, Parkville, Victoria 3010, Australia

Abstract

Terminal velocity of liquid drops is one of the key parameters in liquid-liquid extraction column design. It is important in determining residence time, droplet lifetime, and mass transfer rate. In present paper, the rising behavior of a single drops are investigated in a low interfacial tension system by high speed camera. An n-butanol/water system was used as test system. Correlations for terminal velocity were evaluated and compared, both explicitly and implicitly. Moreover, the influence of salt addition in aqueous phase was also studied, including salt concentrations and types. A Weber-Reynolds correlation was derived on the basis of experimental data. Drag coefficient was then calculated and showed a good agreement compared to the correlations in literatures.

Keywords: terminal drop rise velocity, low interfacial tension system, liquid-liquid extraction

1. Introduction

Liquid-liquid extraction plays an important role in petrochemical, pharmaceutical, hydrometallurgical, as well as post-processing in nuclear industry (Müller et al., 2008). It is a complicated process due to droplets dynamic behavior, including drop rising, breakage, coalescence and mass transfer characteristics (Kopriwa et al., 2012). One of the most fundamental behaviors is single drop rising in a quiescent ambient fluid, which influences the residence time of droplet in an extraction apparatus and affects the overall mass transfer rate subsequently (Kalem et al., 2010). This process is governed by physical properties of the two immiscible phases and is sensitive to contaminations, like ions, surfactants (Edge and Grant, 1972; Griffith, 1962; Leven and Newman, 1999; Li et al., 2003) or solid particles, which are usually unavoidable in industrial operations.

Terminal velocity and drag coefficient of a rising drop are the important parameters and unlike rigid particles, fluid particles rise with fully mobile interface, which can be divided into several periods (Wegener et al., 2014). When diameters are relatively small, drops behave like rigid sphere. As the droplets become larger, inner circulation within droplets occurs, then the droplets enter in a transition stage. During this stage, droplets change their shape and reach maximum terminal velocity and minimum drag coefficient as the diameter increase. As drop diameter increases further, droplets begin to oscillate and deform, resulting in more resistance to motion, therefore slightly reducing the terminal velocity.

In order to determine the terminal velocity of a rising drop, an analytical solution for Navier-Stokes equations was derived by Hadamard (Hadamard, 1911) and Rybczynski (Rybczynski, 1911) which is applicable only for creeping flows ($Re<1$). For higher Re, correlations or models are developed to evaluate terminal velocity for a given system. There are several options:

(1) Explicit correlation for terminal velocity. In an explicit expression, the terminal velocity is derived by dimensional analysis based on experimental data. Hu and Kintner (Hu and Kintner, 1955) investigated ten organic liquids drops in water. A correlation to predict terminal velocity was proposed based on these test systems except one with very low interfacial tension. Klee and Treybal (Klee and Treybal, 1956) measured the terminal velocity of eleven organic-water systems, covering a wide range of physical properties. By considering velocity-diameter curve as two separate regions, the terminal velocity can be obtained for each region. Thorsen *et al.* (Thorsen et al., 1968) proposed the equation for terminal velocity of circulating and oscillating liquid drops on the basis of seven high interfacial tension systems with extreme care to avoid contamination. A comparison was made with Hu-Kintner correlation, it was found that the previous one was not generally valid for system for highly purified liquids. Grace *et al.* (Grace et al., 1976) presented an explicit equations for terminal velocity by applying three previous types of correlation to a large number of experimental data. This correlation was suggested to be applied in the situation where surface-active contamination was inevitable. Henschke *et al.* (Henschke, 2003) considered different correlations for all droplet rising regions and combined them by crossover functions, resulting in a single model which intends to predict terminal velocities over the entire diameter range. These crossover functions add more complexity to the equations and at least three parameters need to be determined based from experimental data for a given system.

(2) Implicit correlation of terminal velocity. Unlike explicit correlations which present a function of $v_t=f(d_e)$, the terminal velocity can only be calculated through an indirect way from $C_D=f(Re)$. A large number of correlations have been proposed in the past few decades, including Hamielec (Hamielec et al., 1963), Saboni and Alexandrova (Saboni and Alexandrova, 2002), Brauer (Brauer, 1979), Polyanin (Polyanin et al., 2001) and so on. However, these correlations were confined into certain range of Reynolds number and some were restricted to spherical drop only, which limit their application. In practice, the terminal velocity has to be calculated by an iteration way. (Wegener et al., 2014)

(3) Generalized graphical correlation in terms of Eo-Re-Mo. These can be applied for preliminary rough estimation of terminal velocity as well as the shape regime. However, as suggested by Clift *et al.* (Clift et al., 1978), since the viscosity of dispersed phase is not considered in any of the three parameters, very pure systems or larger fluid particles in high Morton liquids are not covered in the diagram.

Although different approaches have been adopted for terminal velocity, few of them are valid in low interfacial tension system. In addition, contaminations like surfactants have been taken into consideration, but limited work has been done to determine the influence caused by simple ions such as sodium chloride. Gebauer (Gebauer, 2018) investigated five different types of salts with 0.1M in continuous phase. His work revealed that a toluene drop was slowed down because the addition of salt. Also in toluene-water test system, Chen *et al.* (Chen et al., 2010) found that the terminal velocity was increased as the salt concentration increased from 0.01M to 2M. Zameek *et al.* (Zameek et al., 2016) derived the same trend as Chen *et al.*, they studied the single crude oil drop rising in electrolytes with low, moderate and high concentration. It seems that opposite conclusions were derived for addition of salt. Therefore, further work is needed to investigate the salt effects, especially in low interfacial tension system.

In this study, single drop rising in low interfacial tension system (i.e. butanol-water system) was recorded by high speed camera to obtain terminal velocity. Then the terminal velocities were

compared to the predictions by correlations from literature, both explicitly and implicitly. Furthermore, salt effects were determined by adding different salts with various concentrations into continuous phase. Finally, Re-We-Mo correlation was developed on the basis of experimental data, which was applied to predict drag coefficient for the low interfacial system.

2. Materials and Methods

To observe single drop rising, a column filled with continuous phase is commonly utilized with dispersed phase injected from bottom (Bhavasar et al., 1996; Kamp and Kraume, 2014). Droplets are recorded by high speed camera to estimate the terminal velocity as well as shape information.

2.1 Test system

As proposed by European Federation of Chemical Engineering (EFCE) (Misek et al., 1985), n-butanol/water was chosen as the standard low interfacial tension system in this study. Ultrapure water, with a conductivity less than <0.05 μS/cm, was degassed to eliminate the influence of solute gases. N-butanol with analytical-reagent grade was used to minimize contaminations. Since n-butanol is moderately soluble in water, the two phases were mutually saturated in a stirred tank before experiment to avoid additional mass transfer.

Physical properties of the two phases are summarized in Table 1. To explore the influence of salt ions, salt with certain concentration was firstly dissolved in ultrapure water. After fully dissolved, the salt solution was then mutually saturated with n-butanol as the standard system.

Table 1 - Physical properties of saturated n-butanol/water system

		Density (kg/m^3)	Viscosity (mPa·s)	Interfacial tension (mN/m)
Continuous phase	water	992.9	1.69	1.50
Disperse phase	n-Butanol	820.54	3.58	

Note: Density is calculated by measuring the mass over a specific volume of liquid; the viscosity is measured by viscometer; the interfacial tension is measured by pendant drop method.

Table 2 - Experimental Materials

Salt type	Purity	Company
NaCl	A.R.	Beijing Chemical Works
Na_2SO_4	A.R.	Beijing Chemical Works
NaAc	A.R.	Beijing Chemical Works
NaI	A.R.	Macklin
$MgCl_2·6H_2O$	A.R.	Tianjin Guangfu Technology Development Company
$MgSO_4·7H_2O$	A.R.	Beijing Tongguang Fine Chemicals Company
$AlCl_3·6H_2O$	A.R.	Beijing Tongguang Fine Chemicals Company

2.2 Experimental setup

The Experimental setup is shown in Fig. 1 (1) is a small scale glass made measurement cell with diameter 80mm and effective height 180mm. Nozzle (2) made of stainless steel was located at the bottom of the column and connected to a syringe pump (8) by PTFE tubing (12). Inner

diameter of nozzle varies from 0.13mm to 2.40mm.

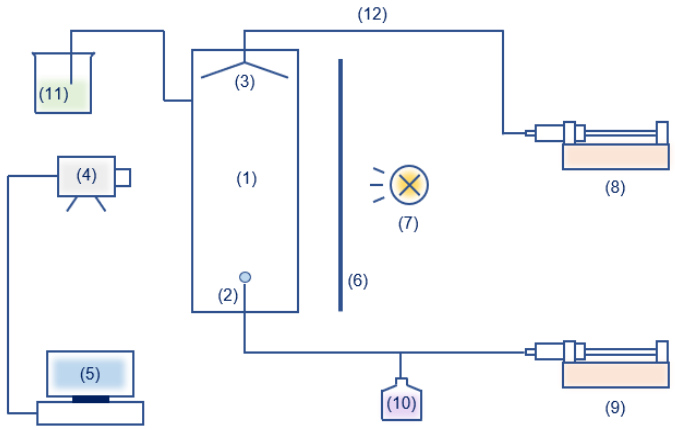

(1) Glass column, (2) stainless steel nozzle, (3) funnel, (4) high speed camera, (5) computer, (6) soft light curtain, (7) illumination system, (8)(9) syringe pump, (10) disperse phase tank, (11) continuous phase tank, (12) PTFE tubing

Fig. 1 - Experimental setup

As the experiment were carried out in containers of finite dimensions, wall effects may exist greater of lesser extent. To estimate wall effect, a new diameter ratio is defined as in literature (Clift et al., 1978):

$$\lambda = \frac{d_e}{D} \tag{1}$$

The following conditions should be satisfied if wall effects are negligible:

$$\begin{gathered} \mathrm{Re} \leq 0.1 \quad \lambda \leq 0.06 \\ 0.1 < \mathrm{Re} \leq 100 \quad \lambda \leq 0.08 + 0.02 \log_{10} Re \\ \mathrm{Re} \geq 100 \quad \lambda \leq 0.12 \end{gathered} \tag{2}$$

Take the standard test system as an example, λ ranges between 0.014 and 0.025, which is far lower than the range of $0.08 + 0.02 \log_{10} Re$ from 0.105 to 0.115, which means that the wall effect has negligible influence less than 2%. Other systems were tested in the same way. Therefore, single drop rising in the test cell are dominated by gravity force, buoyancy force and drag force, where wall effects caused by containers can be ignored.

2.3 Experimental procedure

To keep the test system extremely pure without contaminations, a cleaning procedure has been performed before each test series. All containers including column, tanks, tubing and syringes were cleaned and rinsed at least three times. During the experiment, the motion of droplet was tracked by high speed camera device. A Photon FASTCAM Mini WX50 high-speed camera (4) has been used (2000fps, 1024×1024 pixels resolution). LED light (7) was placed against the high-speed camera with a soft light curtain (6) in between to provide sufficient light for recording. The entire trajectory of droplet can be captured, and images were transferred from camera and saved in computer (5). For each nozzle, at least ten single drops were recorded and then averaged in the following analysis. After the experiment, the organic phase was collected at the funnel (3) and then extracted by syringe pump for disposal.

2.4 Image analysis

For the analysis of the experimental data, image processing was done by software ImageJ 1.52a. The images were analyzed through several procedures to derive (1) drop diameter, (2) drop rise velocity and (3) drop aspect ratio. (ImageJ, 2012; Quinn et al., 2014)

(1) Drop diameter

The equivalent diameter which has same surface area as particle was calculated by the semi major (a) and minor (b) axes of the fitted ellipse to the projected drop area.

$$d_e = a^{1/2} b^{1/2} \tag{3}$$

(2) Drop rise velocity

The vertical displacement of the drop center can be tracked by the software. Therefore, the rise velocity was calculated from displacement difference (Δh) between two consecutive frames. Since the time internal between two frames was very short, the calculated velocity can be regarded as the instantaneous velocity.

$$v_{ins} = \frac{\Delta h}{(1/fps)} \tag{4}$$

As the drop was released from nozzle, it accelerated at a short time to reach its terminal velocity. In this study, the velocity fluctuations within average ±5% were considered as steady state.

3. Results and Discussion

When the standard low interfacial tension system was chosen as the test system, correlations to predict terminal velocity should be applied with caution (Wegener et al., 2014). This is probably due to the higher viscosity ratio with high absolute viscosities combined with very low interfacial tension (Bäumler et al., 2011). Despite these factors, refractive index of butanol is not much higher than water and droplets start to deform at a relatively small diameter, which may add difficulties in image analysis stage. Considering this, correlations from literature were evaluated and compared.

3.1 Terminal velocity

Correlations for terminal velocity were evaluated both explicitly and implicitly. For implicit correlation given as $C_D = f(Re)$, the application range of Reynolds number should be considered carefully.

3.1.1 Explicit correlation

Some of the existing explicit correlations are summarized as Table 3.

Table 3 - Explicit correlations in literatures

Author(s)	Time	Correlation	Description	Equation
Klee *et al.*(Klee and Treybal, 1956)	1956	$v_{t1} = 38.3\rho_c^{-0.45} \triangle \rho^{0.58} \mu_c^{-0.11} {d_e}^{0.70}$ $v_{t2} = 17.6\rho_c^{-0.55} \triangle \rho^{0.28} \mu_c^{0.10} \sigma^{0.18}$	Applicable in low interfacial tension system	(5)

Thorsen *et al.*(Thorsen et al., 1968)	1968	$v_t = \frac{6.8}{1.65 - \frac{\triangle \rho}{\rho_d}} \frac{\sqrt{\frac{\sigma}{3\rho_d + 2\rho_c}}}{\sqrt{d_e}}$	High interfacial tension system without contamination	(6)
Grace *et al.*(Grace et al., 1976)	1976	$v_t = \frac{\mu_c}{\rho_c d_e} Mo^{-0.149}(J - 0.857)$ for $Mo < 10^{-3}, E\ddot{o} < 40$ and $Re > 1$ $\mathrm{J} = 0.94H^{0.757} \quad for\ 2 < H \leq 59.3$ $\mathrm{J} = 3.42H^{0.441} \quad for\ H > 59.3$ $H = \frac{4}{3} E\ddot{o} Mo^{-0.149} \left(\frac{\mu_c}{\mu_w}\right)^{-0.14}$ $(\mu_w = 9 \times 10^{-4}\ Nsm^{-2})$	System with contamination	(7)
Henschke (Henschke, 2003)	2003	$v_t = \frac{v_{\infty,oscillating\ or\ deformed} v_{\infty,spherical}}{(v^{p_3}_{\infty,oscillating\ or\ deformed} + v^{p_3}_{\infty,spherical})^{1/p_3}}$ $v_{\infty,spherical} = \frac{Re_{\infty,spherical}\mu_c}{\rho_c d}$ $\begin{cases} Re_{\infty,spherical} = (1 - f_1^*)Re_{\infty,rigid} + f_1^* Re_{\infty,ideally\ mobile} \\ Re_{\infty,rigid} = \frac{\rho_c v_\infty d}{\mu_c} \\ Re_{\infty,ideally\ mobile} = \frac{Ar}{p_5(0.065Ar + 1)^{1/6}} \\ C_D = \frac{432}{Ar} + \frac{20}{Ar^{1/3}} + \frac{0.51Ar^{\frac{1}{3}}}{140 + Ar^{1/3}} \\ f_1^* = 2(K_{HR}^* - 1) \quad K_{HR}^* = \frac{3(\mu_c + \mu_d/f_2)}{2\mu_c + 3\,\mu_d/f_2} \quad f_2 = 1 - \frac{1}{1 + (d/p_1)^{p_4}} \end{cases}$ $v_{\infty,oscillating\ or\ deformed} = (v^8_{\infty,oscillating} + v^8_{\infty,deformed})^{1/8}$ $\begin{cases} v_{\infty,oscillating} = \sqrt{\frac{2p_2\sigma}{\rho_c d}} \\ v_{\infty,deformed} = \sqrt{\frac{\triangle \rho g d}{2\rho_c}} \end{cases}$ Details also see Reference (Adekojo Waheed et al., 2004; Adinata, 2011)	Parameters should be fitted based on experimental data	(8)

Fig. 2 (a) shows how the terminal velocity varies with drop diameter. Experimental data in this study were well consistent with the simulation result for the same system from literature (Engberg and Kenig, 2014). Models proposed by Henschke (Henschke, 2003) was able to predict the terminal velocity over the whole drop diameter range and are applicable for low interfacial tension systems. However, five parameters were involved in this model and needed to be fitted (p_1=1.28, p_2=4, p_3=2.471, p_4=1.594 and p_5=1.842). Grace model (Grace et al., 1976) gave prediction with deviations because the test system were kept extremely clean without any contamination. Although Klee *et al.* (Klee and Treybal, 1956) derived their correlation covering a wide range of interfacial tension (from 0.3 to 42.4 mPa·s), it seemed that it presented the

predictions with errors. Correlation by Thorsen *et al.* (Thorsen et al., 1968) was proposed for the high interfacial tension system with drop oscillation, which was not suitable for low interfacial system with small diameters.

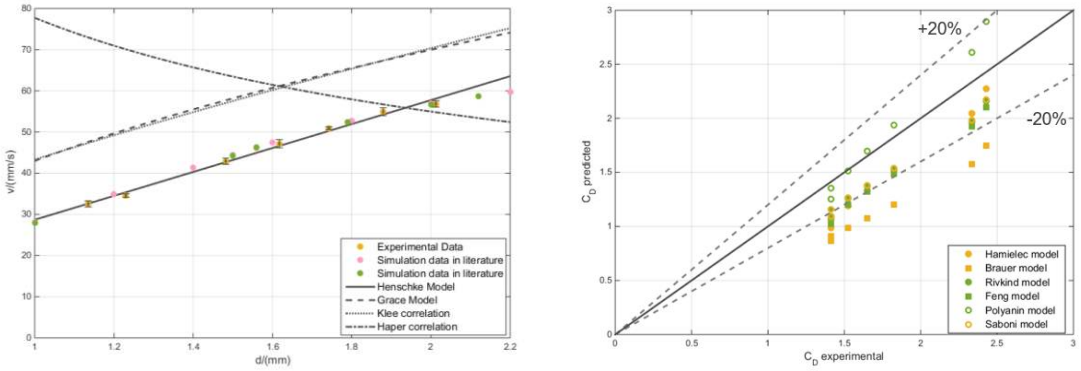

(a) (b)

Fig. 2 Prediction of terminal velocity and drag coefficient

((a) terminal velocity predicted by explicit correlations and models; (b) Drag coefficient predicted by correlations)

3.1.2 Implicit correlation

$C_D = f(Re)$ gave an implicit way to plot terminal velocity versus drop diameter by iteration method. Several correlations from literatures were compared in this section, as summarized in Table 4.

Table 4 - Drag coefficient correlations in literature

Authors	Year	Correlation	Application	Re range	Equation
Hamielec *et al.*(Hamielec et al., 1963)	1963	$C_D = \frac{3.05(783\mu^{*2} + 2142\mu^* + 1080)}{(60 + 29\mu^*)(4 + 3\mu^*)Re^{0.74}}$	Drop	$4 < Re < 100$	(9)
Brauer *et al.*(Brauer, 1979)	1973	$C_D = \frac{16}{Re} + \frac{14.9}{Re^{0.78}}\left(\frac{1}{1 + 10Re^{-0.6}}\right)$	Drop and bubble	$Re < 3 \times 10^5$	(10)
Feng *et al.*(Feng and Michaelides, 2001)	2001	$C_D = \frac{2 - \mu^*}{2}\left[\frac{48}{Re}\left(1 + \frac{2.21}{Re^{1/2}} - \frac{2.14}{Re}\right) + \frac{4\mu^*}{6 + \mu^*}\left(17 \times Re^{-2/3}\right)\right]$	Drop	$0.1 < Re < 10$	(11)
Polyanin *et al.*(Polyanin et al., 2001)	2002	$C_D = \frac{1.83(783\mu^{*2} + 2142\mu^* + 1080)}{(60 + 29\mu^*)(4 + 3\mu^*)} Re^{-0.74}$	Drop	$2 < Re < 50$	(12)
Saboni *et al.*(Saboni and Alexandrova, 2002)	2002	$C_D = \frac{\left[\mu^*\left(\frac{24}{Re} + \frac{4}{Re^{1/3}}\right) + \frac{14.9}{Re^{0.78}}\right]Re^2 + 40\frac{3\mu^* + 2}{Re} + 15\mu^* + 10}{(1 + \mu^*)(5 + Re^2)}$	Drop, bubble and solid particle	$0.01 \leq Re < 400$	(13)

Drag coefficient predicted by these correlations are shown in Fig. 2 (b). All these correlations

were unable to accurately predict the data from low interfacial systems, some predictions were even outside 20% range. It seemed that these $C_D = f(Re)$ correlations were less accurate for low interfacial tension case.

Since drop diameter and terminal velocity coexist on each side of the correlations, the terminal velocity has to be calculated by an iteration procedure. Each of the correlation is validated on specific Reynolds number range, it is necessary to consider the application range and introduce Reynolds number range to the plot.

Traditionally, to calculate the terminal velocity from C_D-Re correlations required a tedious trial-and-error procedure (Briens, 1991; Haider and Levenspiel, 1989; Song et al., 2017) because v_t was present in both variables. However, in this study, v_t-d_e was first plot in a two-dimensional figure with the help of implicit function plot in MATLAB 2014b. Then the data points were extracted from the two-dimensional figure to calculate Reynolds number correspondingly and plot in three-dimensional way, as shown in Fig. 3 (a). Compared with trial-and-error iteration procedure, this method is more convenient and can avoid large amount of computations.

As is shown in Fig. 3 (b)-(i), two parallel planes represent upper and lower range of Reynolds number, respectively. The curve in between demonstrates the prediction of terminal velocity by the corresponding correlation. Red points are experimental data. The two-dimensional plot can be viewed as projection of points and curve on *xoy* plane. Four correlations are presented here, namely, Hamielec (Hamielec et al., 1963), Saboni and Alexandrova (Saboni and Alexandrova, 2002), Brauer (Brauer, 1979) and Polyanin (Polyanin et al., 2001).

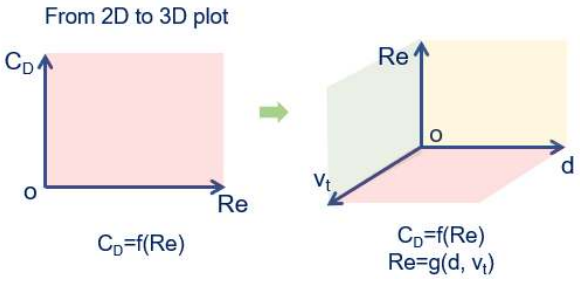

(a)

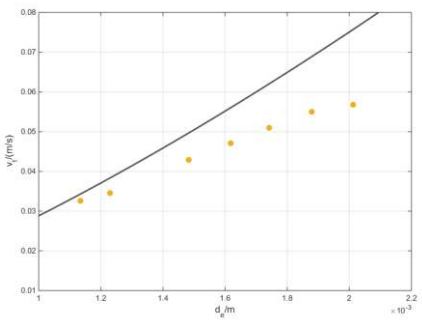

(b)

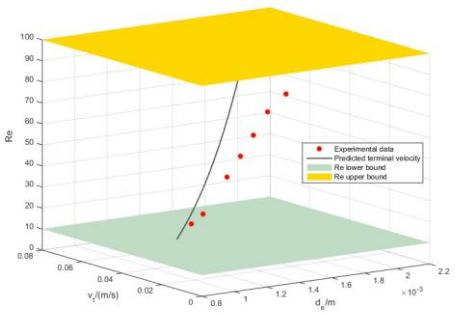

(c)

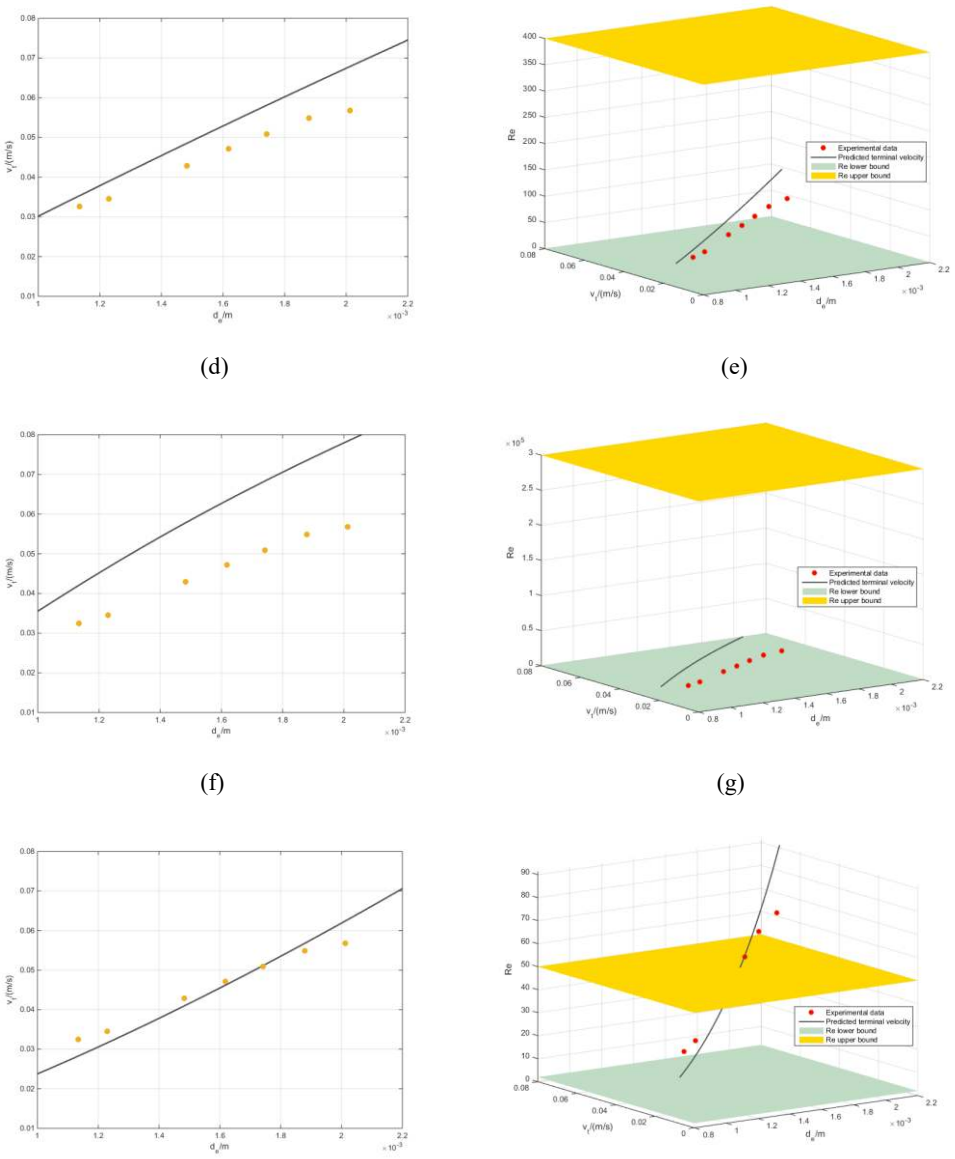

(d) (e)

(f) (g)

(h) (i)

Fig. 3 Terminal velocity predicted from $C_D = f(Re)$ correlation

((a) Sketch of two-dimensional and three-dimensional plot (b),(d),(f),(h) are two dimensional plots; (c),(e),(g),(i), are three dimensional plots involving Reynolds number; (b),(c) Hamielec correlation(Hamielec et al., 1963); (d),(e) Saboni and Alexandrova correlation(Saboni and Alexandrova, 2002); (f),(g) Brauer correlation(Brauer, 1979); (h),(i) Polyanin correlation(Polyanin et al., 2001))

Correlation by Hamielec (Hamielec et al., 1963) can be used within 10< Re<100 for solid particles and drops and bubbles which are only slightly deformed. The effect of dispersed phase viscosity on total drag is presented. However, it can only predicted well in small diameter range, deviations occur as diameter increases, which has been reported by Bäumler (Bäumler et al., 2011). Saboni and Alexandrova (Saboni and Alexandrova, 2002) proposed a correlation for droplet in a range: 0.01< Re<400, viscosity ratio range: 0<μ<1000. The experimental data are all below the predicted terminal velocity, suggesting it may be used with caution in low interfacial tension system. As proposed by Brauer (Brauer, 1979), the correlation is valid in a wide Re range (Re <

300000) for both bubbles and drops. The application range is so broad that deviations may occur in a relative narrow diameter range. Correlation by Polyanin (Polyanin et al., 2001) is validated in a rather narrow Re range (2<Re<50) compared to the former correlation. It shows good agreement with experimental data points. Although several data points exceed the Re range, it can be used as a rough estimation.

3.2 Salt effect on drop motion

The addition of salt changes the physical properties of the system and influences the hydrodynamic behavior of droplet consequently. In this section, the influence of salt concentration and type were investigated.

3.2.1 Change of physical properties

When salt is added into the continuous phase, physical properties changes of the system arises from three aspects: density difference ($\triangle\rho$), interfacial tension (σ) and viscosity of continuous phase (ρ_c). Among these three changes, change of density difference is obvious and the other two changes can be illustrated from a molecular perspective. A well-known series to rank the relative influence of salt ions on physical behavior of aqueous solution is the Hofmeister series (Cacace et al., 1997; Zhang and Cremer, 2006), which was originally used to describe the ability for stabilizing proteins. A theory accounting for this is the ions contribute to "making" or "breaking" bulk water structure. In general, the trend for anions is more pronounced than for cations. The typical order of Hofmeister series are:

For anions, $SO_4^{2-} > HPO_4^{2-} > CH_3COO^- > Cl^- > NO_3^- > ClO_3^- > I^- > ClO_4^- > SCN^-$

For cations, $NH_4^+ > K^+ > Na^+ > Li^+ > Mg^{2+} > Ca^{2+}$

Complex changes for drop motion will be caused by addition of ions and sometimes the changes may lead to opposite contributions. As shown in Fig. 4, with the addition of salt and increase of salt concentration, density difference, viscosity and interfacial tension increase in most cases. (Except for NaI solution, where iodide is attracted to the interface (Lima et al., 2013), decreases the interfacial tension as the concentration increases) However, as can be concluded from literature (Engberg and Kenig, 2014; Huang and Wang, 2018), the increase of $\triangle\rho$ and σ will increase the terminal velocity while increase of ρ_c will slow down the motion. Since the physical properties play a decisive role on the terminal velocity, it is necessary to combine all changes together for analysis.

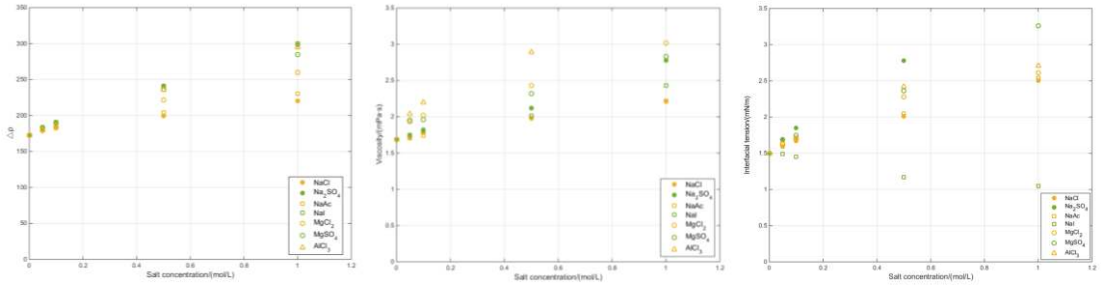

(a) (b) (c)

Fig. 4 - Physical properties varies with salt concentration

((a) density difference of the two phases; (b) viscosity of the continuous phase; (c) interfacial tension)

3.2.2 Influence of salt concentration

Four concentrations of salt solution were tested in this study, i.e. 0.05mol/L, 0.1 mol/L, 0.5 mol/L and 1 mol/L. From a general view in Figure 5 (a) and (b), the terminal velocity increases with concentration. When the concentration is low, like 0.05mol/L or 0.1 mol/L, the increase of terminal velocity is not obvious. However, as the concentration increases increased terminal velocity becomes apparent and the trend is more obvious for Na_2SO_4 than for NaCl.

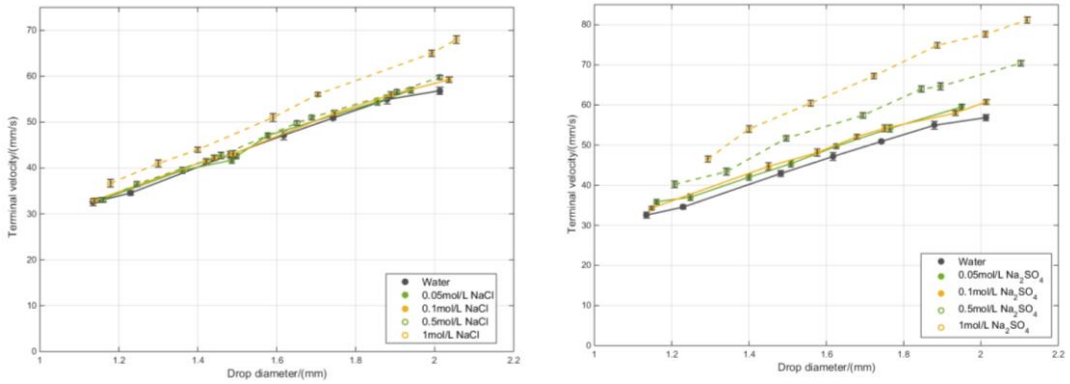

(a) (b)

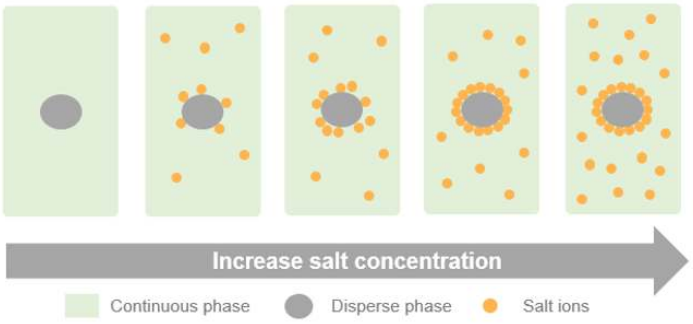

(c)

Fig. 5 Influence of salt concentration on terminal velocity

((a) Salt type: NaCl; (b) Salt type: Na_2SO_4 (c) Sketch of increasing salt concentration)

This can be explained by this, as Fig.5 (c) shows: when the salt concentration is low (e.g. <0.1mol/L), ions absorb at the interface and slightly decrease the interfacial tension, which blocks the inner circulation of the droplet. In this case, the terminal velocities of droplet slow down or remain little change. This is consistent with the conclusions made by Gebauer (Gebauer, 2018). As the concentration increase, the interface becomes saturated with ions and subsequently addition of salt increases the bulk concentration. As a result, increase of density difference becomes the major factor to influence terminal velocity. Therefore, terminal velocity increase obviously at high concentrations, which also accounts for the same trend in literature (Chen et al., 2010). But the difference is that the butanol/water system shows a very small variation at low concentration due to limit interfacial tension change.

3.2.3 Influence of salt type

As mentioned before, the increase of terminal velocity is more apparent for Na_2SO_4 than

NaCl, which suggests the salt type could make a difference. Here, a specific nozzle was chosen with inner diameter of 2.7mm. The terminal velocities at various concentrations are summarized in histogram as shown in Fig. 6.

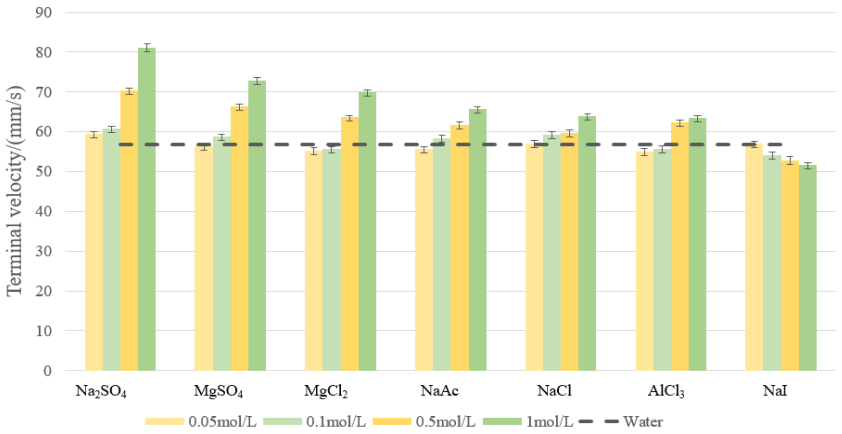

Fig. 6 Influence of salt type and concentration on terminal velocity

For the influence of anions, it reveals that the ability to influence terminal velocity ranks: SO_4^{2-}>Ac^-≈Cl^-> I^-, which is consistent with Hofmeister series. It can be illustrated from both the influence of density difference as well as interfacial tension of the system. For NaI, although the density difference was increased after the addition of ions, the terminal velocity decreases when concentration increases. It is because I^- break the structure of water and reduce the interfacial tension, which consequently decreases the drop diameter and results in a lower terminal velocity. For the influence of cations, there seems no obvious trend, like Al^{3+}> Mg^{2+}> Na^+. This may be attributed to the viscosity increase becoming dominated when $AlCl_3$ added into the solution, which slows down the terminal velocity. Therefore, terminal velocity influenced by ions is a complicated case and changes in physical properties should be examined carefully.

3.3 Weber-Reynolds correlation

For rising bubbles in clean liquids, Maxworthy *et al.* (Maxworthy et al., 1996) proposed a correlation for Weber number versus Reynolds number followed by a power law

$$We = f(Mo)Re^{5/3} \tag{14}$$

Where f(Mo) was found by cross-plotting the experimental data:

$$f(Mo) = 0.526Mo^{0.358} \tag{15}$$

And drag coefficient can be derived:

$$C_D = \frac{4Eo}{3We} = \frac{4}{3f(Mo)}\frac{Eo}{Re^{5/3}} \tag{16}$$

It is valid for low values of Morton number (Mo<3.8×10^{-4}) and can be applied to where extreme precision is not required. Raymond *et al.* (Raymond and Rosant, 2000) followed the same procedure and correlated their data to obtain the function f(Mo) as

$$f(Mo) = 0.42Mo^{0.35} \tag{17}$$

Good agreement was found and shown that the correlation is also valid for large Morton numbers, Mo=9×10^{-7}-7. More recently, Cano-Lozano *et al.* (Cano-Lozano et al., 2015) correlated Reynolds number with Weber number in such a way:

$$Re = 2.05We^{2/3}Mo^{-1/5} \tag{18}$$

It was noticed that the experimental data are consistent within the correlation in a stable rectilinear regime, but discrepancies were detected at high Reynold numbers.

For liquid-liquid system, attempts has been made by Wegener *et al.* (Wegener et al., 2009) in toluene-water system. They utilized the same correlation by Maxworthy *et al.* (Maxworthy et al., 1996) without any changes. Up to the minimum drag point, the correlation can be used for a rough approximation. However, the correlation is not useful for higher Reynolds numbers where deviations can up to 150%.

Following the suggestion of Raymond and Rosant (Raymond and Rosant, 2000), all the experimental data are firstly plotted in We-Re diagram with double logarithmic coordinates and are fitted by a power law. Then function of Mo is determined by curve fitting. Finally, correlation for this study is derived:

$$We = 0.4015Mo^{0.3243}Re^{1.526} \tag{19}$$

And correlation for drag coefficient:

$$C_D = \frac{4Eo}{1.2045Mo^{0.3243}Re^{1.526}} \tag{20}$$

A comparison is made between various correlations in Fig. 7. It can be observed that all prediction values by the correlation falls within ±20%. Other correlations show larger deviations.

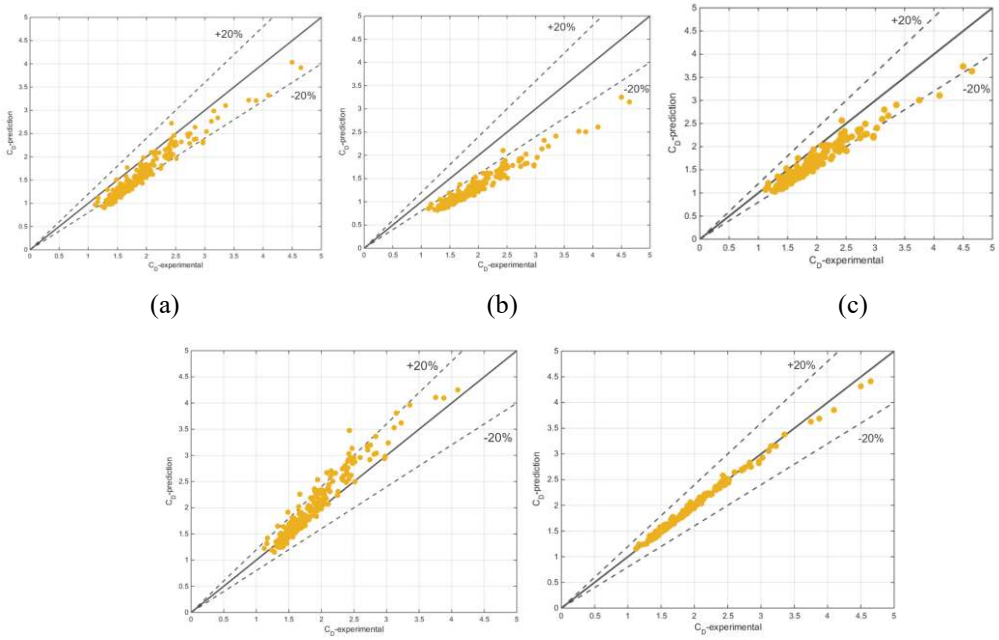

(a) (b) (c)

(d) (e)

Fig. 7 Drag coefficient predicted by proposed correlation and correlations from literature

((a) Hamielec correlation(Hamielec et al., 1963); (b) Brauer correlation(Brauer, 1979); (c) Saboni and Alexandrova correlation(Saboni and Alexandrova, 2002); (d) Polyanin correlation(Polyanin et al., 2001))

The correlation is also tested in high interfacial tension system, as shown in Fig.8. Compared with previous correlations in literature, this correlation can reduce the mean absolute deviation

from 44.46% to 16.32%. Although derived on the basis of data from low interfacial tension system, the correlation can also be extended to high interfacial tension system. However, deviations still arises when the Reynolds numbers are high, as mentioned by Wegener *et al.* (Wegener et al., 2009)

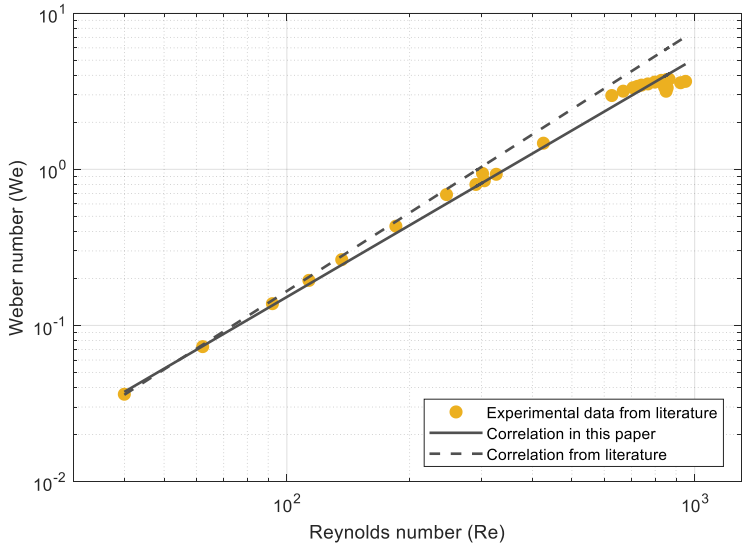

Fig.8 Correlation tested in high interfacial tension system
(Experimental data and correlation are from Wegener (Wegener et al., 2009))

4. Conclusions

In this paper, hydrodynamic behavior of an n-butanol drop rising in water as well as in salt solution have been investigated experimentally.

The rising velocity and shape information were recorded by high speed camera. Various correlations for the terminal velocity were evaluated and compared. Explicit v_t-d_e correlations were shown not to be accurate for this system with the exception of the model by Henschke which showed agreement with the experimental data, but relies on the experimental data to determine parameters in model. For implicit v_t-d_e relationship derived from C_D=f(Re), application range of Re should be considered carefully. Correlations are evaluated and compared in a v_t-d_e-Re three-dimensional plot these.

The influence caused by salt ions was also investigated. The addition of salt changed the test system in three aspects: density difference, viscosity and interfacial tension. When the salt concentration is low, ions absorb at the interface and thus slow down the inner circulation and terminal velocity. But this change is small for low interfacial tension systems. As the concentration of added salt increases, the absorption of ions at the interface becomes saturated. In this case, density increase in bulk solution is the dominated factor, which increases the terminal velocity. Physical properties changed by different types of ions follows the Hofmeister series. Results shows that anions exhibit more influence than cations. Influences by ions are complicated and physical properties change should be considered carefully.

A We-Re correlation was proposed for all the experimental liquid-liquid systems in this study. It was interesting to find that the new correlation could be extended to high interfacial tension system. However, small deviations arise when Re numbers are high.

Low interfacial tension system is of great interest for bio-extraction process such as aqueous

two-phase systems. So future work is needed on the influence of this on mass transfer rates. In addition, contaminations caused by coexistence of salt ions and surfactants should be studied in detail.

Nomenclature

a	Major axis of the fitted ellipse, m
b	Minor axis of the fitted ellipse, m
C_D	Drag coefficient
d_e	Equivalent drop diameter, m
D	Diameter of the container, m
Eo	Eötvös number
fps	Frames per second, s^{-1}
λ	Parameter to estimate wall effects
Mo	Morton number
Re	Reynolds number
t	Time, s
μ^*	Viscosity ratio
v_t	Terminal velocity, m/s
v_{ins}	Instantaneous velocity, m/s
We	Weber number

Acknowledgements

This research was carried out under the National Natural Science Foundation of China (21636004), the National Safety Academy Foundation (U1530107), the National Key Basic Research Program of China (No.2012CBA01203) in the State Key Laboratory of Chemical Engineering of Tsinghua University, Beijing, China. The authors gratefully acknowledge these grants.

References

Adekojo Waheed, M., Henschke, M., Pfennig, A., 2004. Simulating sedimentation of liquid drops. Int. J. Numer. Methods Eng. 59, 1821-1837.

Adinata, D., 2011. Single-Drop Based Modelling of Solvent Extraction in High-Viscosity Systems. RWTH Aachen University, Germany.

Bäumler, K., Wegener, M., Paschedag, A.R., Bänsch, E., 2011. Drop rise velocities and fluid dynamic behavior in standard test systems for liquid/liquid extraction—experimental and numerical investigations. Chem. Eng. Sci. 66, 426-439.

Bhavasar, P.M., Jafarabad, K.R., Pandit, A.B., Sawant, S.B., Joshi, J.B., 1996. Drop Volumes and Terminal Velocities in Aqueous Two Phase Systems. Can. J. Chem. Eng. 74, 852-860.

Brauer, H., 1979. Particle/fluid transport processes, in: Fortschritte in der Verfahrenstechnik, VDI Verlag, Düsseldorf.

Briens, C.L., 1991. Correlation for the direct calculation of the terminal velocity of spherical particles in newtonian and pseu-doplastic (power-law) fluids. Powder Technol. 67, 87-91.

Cacace, M.G., Landau, E.M., Ramsden, J.J., 1997. The Hofmeister series: salt and solvent effects on interfacial phenomena. Q. Rev. Biophys. 30, 241-277.

Cano-Lozano, J.C., Bolaños-Jiménez, R., Gutiérrez-Montes, C., Martínez-Bazán, C., 2015. The use of Volume of Fluid technique to analyze multiphase flows: Specific case of bubble rising in still liquids. Appl. Math. Modell. 39, 3290-3305.

Chen, C. T., Maa, J. R., Yang, Y. M., Chang, C.H., 2010. Salt Effects on Single Aqueous Drops Falling through an Immiscible Organic Liquid. Chem. Eng. Commun. 189, 1297-1313.

Clift, R., Grace, J. R., Weber, M. E., 1978. Bubbles, Drops and Particles. Academic Press New York.

Edge, R. M., Grant, C.D., 1972. The motion of drops in water contaminated with a surface-active agent. Chem. Eng. Sci. 27, 1709-1721.

Engberg, R. F., Kenig, E.Y., 2014. Numerical simulation of rising droplets in liquid–liquid systems: A comparison of continuous and sharp interfacial force models. Int. J. Heat Fluid Flow 50, 16-26.

Feng, Z. G., Michaelides, E. E., 2001. Drag Coefficients of Viscous Spheres at Intermediate and High Reynolds Numbers. J. Fluids Eng. 123, 841-849.

Gebauer, F., 2018. Fundamentals of Binary Droplet Coalescence in Liquid-Liquid Systems. Technischen Universität Kaiserslautern, Germany.

Grace, J.R., Wairegi, T., Nguyen, T.H., 1976. Shapes and Velocities of Single Drops and Bubbles Moving Freely through Immiscible Liquids. Chem. Eng. Res. Des. 54, 167-173.

Griffith, R. M., 1962. The effect of surfactants on the terminal velocity of drops and bubbles. Chem. Eng. Sci. 17, 1057-1070.

Hadamard, J. S., 1911. Mouvement permanent lent d'une sphere liquid et visqueuse dans un liquide visqueux. CR Hebd. Seances Acad. Sci. 152, 1735-1738.

Haider, A., Levenspiel, O., 1989. Drag Coefficient and Terminal Velocity of Spherical and Nonspherical Particles. Powder Technology 58, 63-70.

Hamielec, A. E., Storey, S.H., Whitehead, J.M., 1963. Viscous flow around fluid spheres at intermediate reynolds numbers (II). Can. J. Chem. Eng. 41, 246-251.

Henschke, M., 2003. Auslegung pulsierter Siebboden-Extraktionskolonnen. Shaker Verlag, Germany.

Hu, S., Kintner, R.C., 1955. The Fall of Single Liquid Drops Through Water. AICHE J. 1, 42-48.

Huang, Z.Q., Wang, H., 2018. VOF Simulation Studies on Single Droplet Fluid Dynamic Behavior in Liquid–Liquid Flow Process. J. Chem. Eng. Jpn. 51, 33-48.

ImageJ, 2012. ImageJ User Guide.

Kalem, M., Mehmet, Y. A., Pfennig, A., 2010. Sedimentation Behavior of Droplets for the Reactive Extraction of Zinc with D_2EHPA. AICHE J. 56, 7.

Kamp, J., Kraume, M., 2014. Influence of drop size and superimposed mass transfer on coalescence in liquid/liquid dispersions – Test cell design for single drop investigations. Chem. Eng. Res. Des. 92, 635-643.

Klee, A. J., Treybal, R.E., 1956. Rate of Rise or Fall of Liquid Drops. AICHE J.

Kopriwa, N., Buchbender, F., Ayesterán, J., Kalem, M., Pfennig, A., 2012. A Critical Review of the Application of Drop-Population Balances for the Design of Solvent Extraction Columns: I. Concept of Solving Drop-Population Balances and Modelling Breakage and Coalescence. Solvent Extr. Ion Exch. 30, 683-723.

Leven, M. D., Newman, J., 1999. The Effect of Surfactant on the Terminal and Interfacial Velocities of a Bubble or Drop. AICHE J. 22, 695-701.

Li, X. J., Mao, Z. S., Fei, W. Y., 2003. Effects of surface-active agents on mass transfer of a solute into single

buoyancy driven drops in solvent extraction systems. Chem. Eng. Sci. 58, 3793-3806.

Lima, E. R. A., De Melo, B. M., Baptista, L. T., Paredes, M.L.L., 2013. Specific ion effects on the interfacial tension of water/hydrocarbon systems. Braz. J. Chem. Eng. 30, 55-62.

Müller, E., Berger, R., Blass, E., Sluyts, D., Pfennig, A., 2008. Liquid-Liquid Extraction. Ullmann's Encyclopedia of Industrial Chemistry.

Maxworthy, T., Gnann, C., Kürten, M., Durst, F., 1996. Experiments on the rise of air bubbles in clean viscous liquids. J. Fluid Mech. 321, 421-441.

Misek, T., Berger, R., Schröter, J., 1985. Standard test systems for liquid extraction, EFCE Publ. Ser. No. 46, The Institution of Chemical Engineers, England

Polyanin, A.D., Kutepov, A.M., Kazenin, D.A., Vyazmin, A.V., 2001. Hydrodynamics, mass and heat transfer in chemical engineering. CRC Press.

Quinn, J. J., Maldonado, M., Gomez, C.O., Finch, J.A., 2014. Experimental study on the shape–velocity relationship of an ellipsoidal bubble in inorganic salt solutions. Miner. Eng. 55, 5-10.

Raymond, F., Rosant, J.-M., 2000. A numerical and experimental study of the terminal velocity and shape of bubbles in viscous liquids. Chem. Eng. Sci. 55, 943-955.

Rybczynski, W., 1911. On the translatory motion of a fluid sphere in a viscous medium. Bull. Acad. Sci., Cracow, Series A 40.

Saboni, A., Alexandrova, S., 2002. Numerical study of drag on a fluid sphere. AICHE J. 48, 2992-2994.

Song, X., Xu, Z., Li, G., Pang, Z., Zhu, Z., 2017. A new model for predicting drag coefficient and settling velocity of spherical and non-spherical particle in Newtonian fluid. Powder Technol. 321, 242-250.

Thorsen, G., Stordalen, R.M., Terjesen, S.G., 1968. On the terminal velocity of circulating and oscillating liquid drops. Chem. Eng. Sci. 23, 413-426.

Wegener, M., Kraume, M., Paschedag, A.R., 2009. Terminal and transient drop rise velocity of single toluene droplets in water. AICHE J. 56, 2-10.

Wegener, M., Paul, N., Kraume, M., 2014. Fluid dynamics and mass transfer at single droplets in liquid/liquid systems. Int. J. Heat Mass Transfer 71, 475-495.

Zameek, M.A.Z., Lim, M.W., Lau, E.V., 2016. Terminal Velocity of Heavy Crude Oil in Aqueous Solution: Effects of pH and Salinity. Int. Proc. Chem., Biol. Environ. Eng.

Zhang, Y., Cremer, P.S., 2006. Interactions between macromolecules and ions: The Hofmeister series. Curr. Opin. Chem. Biol. 10, 658-663.

Author/s:
Zhang, J;Wang, Y;Stevens, GW;Fei, W

Title:
An experimental study on single drop rising in a low interfacial tension liquid–liquid system

Date:
2019-08-01

Citation:
Zhang, J., Wang, Y., Stevens, G. W. & Fei, W. (2019). An experimental study on single drop rising in a low interfacial tension liquid–liquid system. Chemical Engineering Research and Design, 148, pp.349-360. https://doi.org/10.1016/j.cherd.2019.06.024.

Persistent Link:
http://hdl.handle.net/11343/241451